Three-Dimensional Structure of the Zinc-Containing Phosphotriesterase with the Bound Substrate Analog Diethyl 4-Methylbenzylphosphonate[†,‡]

Janeen L. Vanhooke,[§] Matthew M. Benning,[§] Frank M. Raushel,[||] and Hazel M. Holden*[,§]

Department of Biochemistry and Institute for Enzyme Research, University of Wisconsin, 1710 University Avenue, Madison, Wisconsin 53705, and Department of Chemistry, Texas A&M University, College Station, Texas 77843

Received February 9, 1996; Revised Manuscript Received March 7, 1996[⊗]

ABSTRACT: Phosphotriesterase from *Pseudomonas diminuta* catalyzes the hydrolysis of paraoxon and related acetylcholinesterase inhibitors with rate enhancements that approach 10^{12}. The enzyme requires a binuclear metal center for activity and as isolated contains 2 equiv of zinc per subunit. Here we describe the three-dimensional structure of the Zn^{2+}/Zn^{2+}-substituted enzyme complexed with the substrate analog diethyl 4-methylbenzylphosphonate. Crystals employed in the investigation belonged to the space group *C*2 with unit cell dimensions of $a = 129.6$ Å, $b = 91.4$ Å, $c = 69.4$ Å, $\beta = 91.9°$, and two subunits in the asymmetric unit. The model was refined by least-squares analysis to a nominal resolution of 2.1 Å and a crystallographic *R*-factor of 15.4% for all measured X-ray data. As in the previously reported structure of the cadmium-containing enzyme, the bridging ligands are a carbamylated lysine residue (Lys 169) and a hydroxide. The zinc ions are separated by 3.3 Å. The more buried zinc ion is surrounded by His 55, His 57, Lys 169, Asp 301, and the bridging hydroxide in a trigonal bipyramidal arrangement as described for the cadmium-substituted enzyme. Unlike the octahedral coordination observed for the more solvent-exposed cadmium ion, however, the second zinc is tetrahedrally ligated to Lys 169, His 201, His 230, and the bridging hydroxide. The diethyl 4-methylbenzylphosphonate occupies a site near the binuclear metal center with the phosphoryl oxygen of the substrate analog situated at 3.5 Å from the more solvent-exposed zinc ion. The aromatic portion of the inhibitor binds in a fairly hydrophobic pocket. A striking feature of the active site pocket is the lack of direct electrostatic interactions between the inhibitor and the protein. This most likely explains the broad substrate specificity exhibited by phosphotriesterase. The position of the inhibitor within the active site suggests that the nucleophile for the hydrolysis reaction is the metal-bound hydroxide.

The phosphotriesterase from *Pseudomonas diminuta* catalyzes, with very high turnover numbers, the hydrolysis of organophosphorus pesticides and nerve agents (Dumas *et al.,* 1989). Typical reactions with the insecticide paraoxon and the nerve agent sarin are as follows:

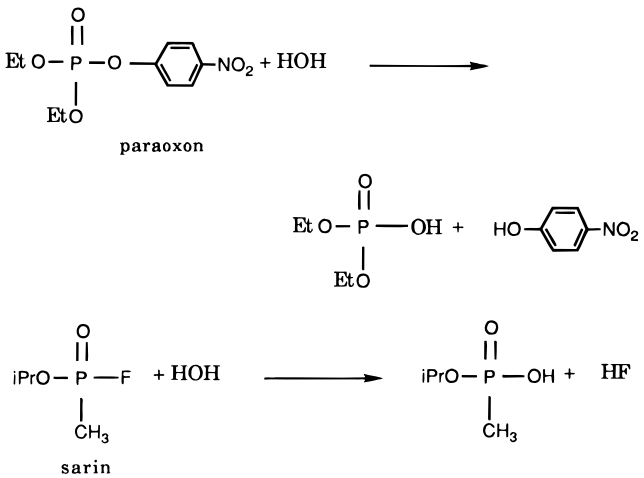

The active site of this remarkable enzyme has been shown to consist of a binuclear metal center that can be assembled in an active configuration with either Zn^{2+}, Mn^{2+}, Co^{2+}, Ni^{2+}, or Cd^{2+} (Omburo *et al.,* 1992). The k_{cat} values for the Zn^{2+}/Zn^{2+}-substituted enzyme are 2100 s^{-1} and 56 s^{-1} with paraoxon and sarin, respectively (Dumas *et al.,* 1990).

Recent NMR, EPR, and X-ray crystallographic investigations have provided a wealth of structural and mechanistic details concerning the active site of phosphotriesterase. ^{113}Cd NMR spectroscopic studies have demonstrated that the two enzyme-bound Cd^{2+} ions are in slightly different chemical environments (Omburo *et al.,* 1993). In addition, EPR spectra of the Mn^{2+}/Mn^{2+}-substituted enzyme have proven that the two metal ions are closely bound and are antiferromagnetically coupled through a common ligand (Chae *et al.,* 1993). Through X-ray crystallographic analysis, the molecular motifs of both the apo- and the cadmium-substituted forms of phosphotriesterase are now known to 2.1 and 2.0 Å resolution, respectively (Benning *et al.,* 1994, 1995). By analysis of the crystalline packing of the apoenzyme, it was shown that the quaternary structure of phosphotriesterase is dimeric rather than monomeric as originally assumed. The structure of the apoenzyme also demonstrated that the overall fold of phosphotriesterase consists of an α/β-barrel with eight strands of parallel β-pleated sheet.

Subsequent studies of the holoenzyme revealed that the active site is located at the C-terminal portion of the β-barrel with the cadmium ions separated by 3.7 Å (Benning *et al.,* 1995). The more buried metal is ligated to His 55, His 57, and Asp 301, while the more solvent-exposed cadmium ion

[†] This research was supported in part by grants from the NIH (GM-33894 to F.M.R. and DK47814 to H.M.H.).

[‡] Coordinates have been deposited in the Brookhaven Protein Data Bank under the filename 1DPM.

* To whom correspondence should be addressed.

[§] University of Wisconsin.

[||] Texas A&M University.

[⊗] Abstract published in *Advance ACS Abstracts,* April 15, 1996.

S0006-2960(96)00325-X CCC: $12.00

Table 1: Intensity Statistics

	resolution range (Å)								
	overall	50.00−4.20	3.33	2.91	2.65	2.46	2.31	2.20	2.10
no. of measurements	41365	5863	5867	5659	5361	5164	4841	4480	4130
completeness of data (%)	88	97	99	96	91	88	83	76	70
average intensity	4000	10000	7742	3623	2139	1496	1192	946	734
average σ	607	701	793	667	544	508	506	488	463
R-factor (%)[a]	6.1	3.5	4.7	7.3	10.2	13.8	16.9	20.5	24.7

[a] $R\text{-factor} = (\Sigma|I - \bar{I}|/\Sigma I) \times 100$.

is coordinated to His 201, His 230, and two water molecules. Additionally, the two metals are bridged together by a hydroxide and a carbamate functional group formed by the reaction of CO_2 and the ϵ-amino group of Lys 169. Quite surprisingly, the overall tertiary fold and the architecture of the binuclear cadmium center of phosphotriesterase resemble those of urease with a binuclear nickel center (Jabri *et al.*, 1995). With the exception of the direct ligands to the metals, urease and phosphotriesterase possess very little amino acid sequence identity. Nevertheless, the close structural resemblance of these two proteins suggests that they may share a common ancestor.

Phosphotriesterase contains up to 2 equiv of zinc per subunit. As indicated above, however, the original three-dimensional model of the holoenzyme determined by X-ray crystallographic analysis was of the cadmium-substituted protein. Phosphotriesterase with zinc bound at the active site has now been crystallized and the structure determined to high resolution. This study highlights the specific differences and similarities at the active site imposed by the binding of alternate metal ions with varying ligation preferences. In addition, the structure reported of the Cd^{2+}/Cd^{2+} protein was determined in the presence of an inert substrate analog, and the inhibitor was found to bind unexpectedly within a hydrophobic region between the two monomers. The structure described here has a substrate analog bound adjacent to the binuclear zinc center. The observed interactions between this substrate analog and the protein provide valuable new information regarding the broad range of substrate specificity exhibited by phosphotriesterase and permit postulation of a chemical mechanism for the hydrolysis reaction.

MATERIALS AND METHODS

Purification and Crystallization Procedures. The enzyme employed for crystallization was purified and reconstituted with Zn^{2+} according to published procedures, dialyzed against 10 mM HEPES, pH 8.5, and concentrated to 11 mg/ml for storage at −135 °C (Omburo *et al.*, 1992). For crystallization trials, the protein was diluted to 5.5 mg/mL in 20 mM HEPES, pH 7.5. Single crystals were grown by the hanging drop method of vapor diffusion at 4 °C. The precipitant solution contained 13% poly(ethylene glycol) 8000, 100 mM CHES (pH 9.0), and 5 mM NaN_3. In addition, 1% diethyl 4-methylbenzylphosphonate was included in the crystallization experiments.

The crystals belonged to the space group *C*2, with unit cell dimensions of $a = 129.6$ Å, $b = 91.4$ Å, $c = 69.4$ Å, $\beta = 91.9°$ and two subunits in the asymmetric unit. Crystal growth was generally complete within 1 week with some crystals achieving maximum dimensions of 0.5 mm × 0.5 mm × 0.2 mm.

Table 2: Least Squares Refinement Statistics

resolution limits (Å)	30.0−2.1
R-factor (%)[a]	15.4
no. of reflections used	41252
no. of protein atoms	5030
no. of solvent atoms	263
weighted root-mean-square deviations from ideality	
bond length (Å)	0.016
bond angle (deg)	2.3
planarity (trigonal) (Å)	0.007
planarity (other planes) (Å)	0.011
torsional angle (deg)[b]	16.5

[a] $R\text{-factor} = \Sigma|F_o - F_c|/\Sigma|F_o|$, where F_o is the observed structure factor amplitude and F_c is the calculated structure factor amplitude. [b] The torsional angles were not restrained during the refinement.

X-ray Data Collection and Processing. For X-ray diffraction experiments, the crystals were mounted in quartz capillary tubes and cooled to 4 °C. A native X-ray data set was collected to 2.1-Å resolution from a single crystal with a Siemens X1000D area detector system. The X-ray source was nickel-filtered Cu Kα radiation from a Rigaku RU200 X-ray generator operated at 50 kV and 90 mA and equipped with double-focusing mirrors. A crystal-to-detector distance of 16 cm was utilized together with a step size of 0.15° per frame.

X-ray data were processed with the X-ray data reduction software package XDS (Kabsch, 1988a,b) and internally scaled with the program XSCALIBRE (Wesenberg and Rayment, unpublished results). Relevant data collection statistics may be found in Table 1. The X-ray data set was 88% complete to 2.1 Å resolution.

Computational Methods. The crystals utilized in this investigation were isomorphous to those previously employed for the structural determination of the Cd^{2+}-substituted enzyme (Benning *et al.*, 1995). As such, the coordinates for the Cd^{2+}/Cd^{2+}-enzyme served as the starting model for the least-squares refinement of the structure reported here. All solvent molecules were deleted from the initial coordinate file. Following several cycles of refinement with the program package TNT (Tronrud *et al.*, 1987) and manual model building with the software FRODO (Jones, 1985), the inhibitor, diethyl 4-methylbenzylphosphonate, was positioned into the electron density map. Four molecules of this inhibitor were observed to bind in the asymmetric unit; two were located at crystalline interfaces and the other two were found near the binuclear metal centers. In addition, 263 water molecules were included in the model. The average temperature factor for the solvent was 33.8 Å^2.

Overall, the electron density was very well-defined with only the following side chains slightly disordered: Asp 35, Arg 36, Arg 67, Arg 89, Arg 96, Arg 118, Glu 263, Lys 294, Arg 319, Arg 331, Arg 356, and Arg 363 in subunit I and Asp 35, Arg 36, Arg 67, Arg 89, Glu 263, Arg 319,

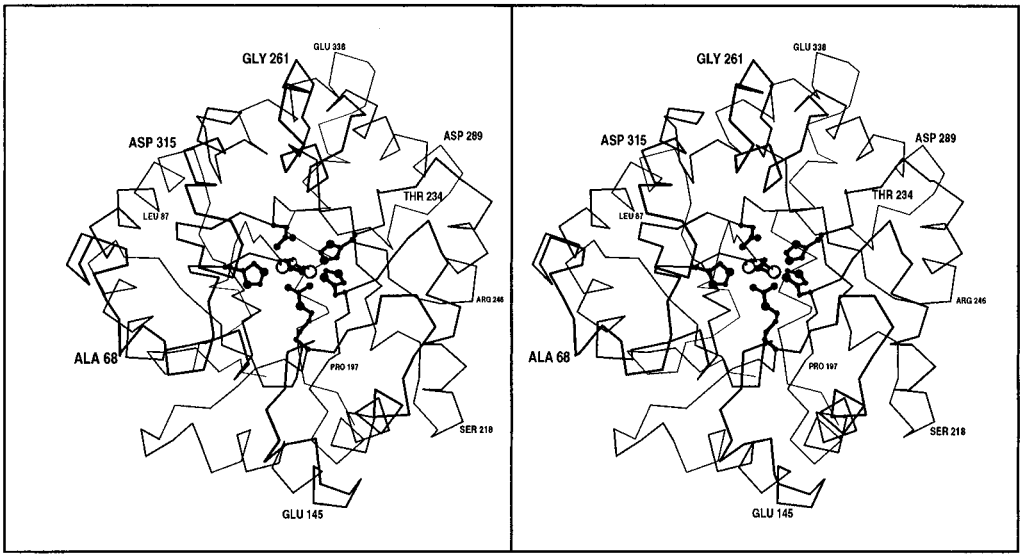

FIGURE 1: α-Carbon trace of one subunit of phosphotriesterase. This figure was prepared with the software package MOLSCRIPT (Kraulis, 1991). The ligands to the binuclear metal center are displayed in a ball-and-stick representation.

Arg 331, Arg 337, Glu 344, and Arg 363 in subunit II. The average *B*-values for all main chain backbone atoms were 21.7 and 20.8 Å^2, for subunits I and II, respectively. A Ramachandran plot of the non-glycinyl main chain dihedral angles revealed only one significant outlier in each subunit: Glu 159 (subunit I) ($\phi = 53.5°$, $\psi = -133.7°$) and Glu 159 (subunit II) ($\phi = 51.8°$, $\psi = -133.3°$). These dihedral angles for Glu 159 were similar to those observed for the Cd^{2+}-containing enzyme and the apoenzyme (Benning *et al.*, 1994, 1995). The reason that Glu 159 adopted such strained ϕ,ψ angles is not clear. Glu 159 is approximately 15 Å from the active site and most likely does not play a role in the catalytic mechanism of the enzyme. The final *R*-factor for all measured X-ray data from 30 to 2.1 Å was 15.4%. Relevant refinement statistics may be found in Table 2. Since the two molecules in the asymmetric unit superimpose with a root-mean-square deviation of 0.16 Å^2 for all main chain backbone atoms, the following discussion will refer only to subunit II. Note, however, that the active sites for the two subunits in the asymmetric unit are identical within experimental error.

RESULTS AND DISCUSSION

An α-carbon trace of one subunit of the zinc-containing phosphotriesterase is shown in Figure 1. The polypeptide chain backbone atoms for the model described here superimpose upon the previously determined Cd^{2+}-containing enzyme structure with a root-mean-square deviation of 0.20 Å. The high degree of three-dimensional similarity between the two forms of the enzyme is not surprising in light of the fact that phosphotriesterase is catalytically active with a variety of divalent metal ions (Omburo *et al.*, 1992). A cartoon of the coordination geometry about the two zinc ions is shown in Figure 2a. For comparison purposes, the coordination geometry of the previously solved Cd^{2+}-containing enzyme is indicated in Figure 2b. In the structure described here, the zinc ions are separated by 3.3 Å. As in the Cd^{2+}-containing enzyme, the bridging ligands for the binuclear metal center are a hydroxide ion and Lys 169, which is carbamylated. Likewise, the more buried zinc ion is coordinated to His 55, His 57, Lys 169, Asp 301, and the

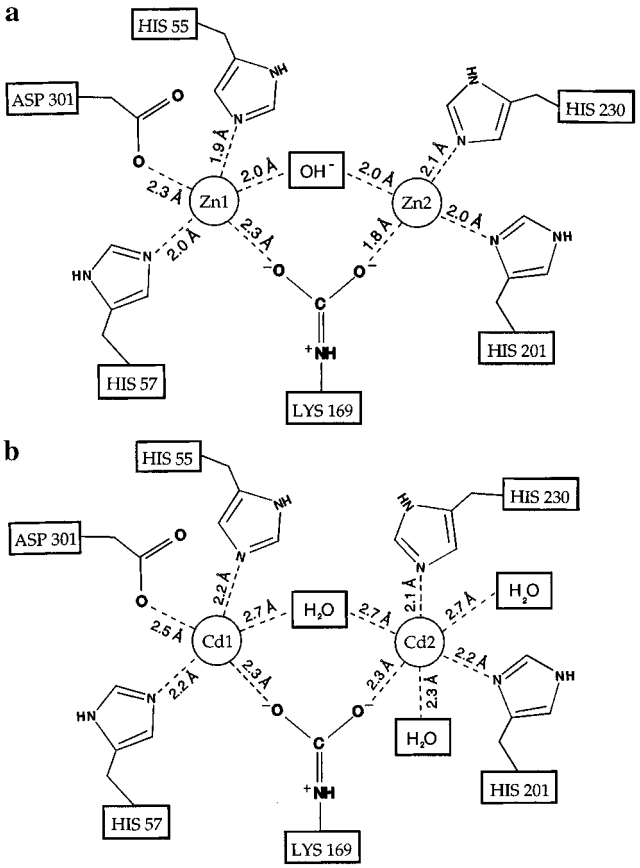

FIGURE 2: Schematic representations of the Zn^{2+}/Zn^{2+} and the Cd^{2+}/Cd^{2+} centers. (a) The bond lengths quoted are those of the average distances observed for the two zinc-containing subunits in the asymmetric unit. The active site residues, the metals, and the inhibitors in the two unique subunits superimpose with a root-mean-square deviation of 0.42 Å. For comparison purposes, the coordination geometry observed in the cadmium-containing phosphotriesterase is shown in (b).

bridging solvent in a trigonal bipyramidal arrangement. The bond lengths between these ligands and the zinc ion are, within experimental error, the same as those observed in the Cd^{2+}/Cd^{2+} protein. One significant difference between the Cd^{2+}- and Zn^{2+}-substituted enzymes occurs in the coordination sphere of the more solvent-exposed cation. In the Cd^{2+}-

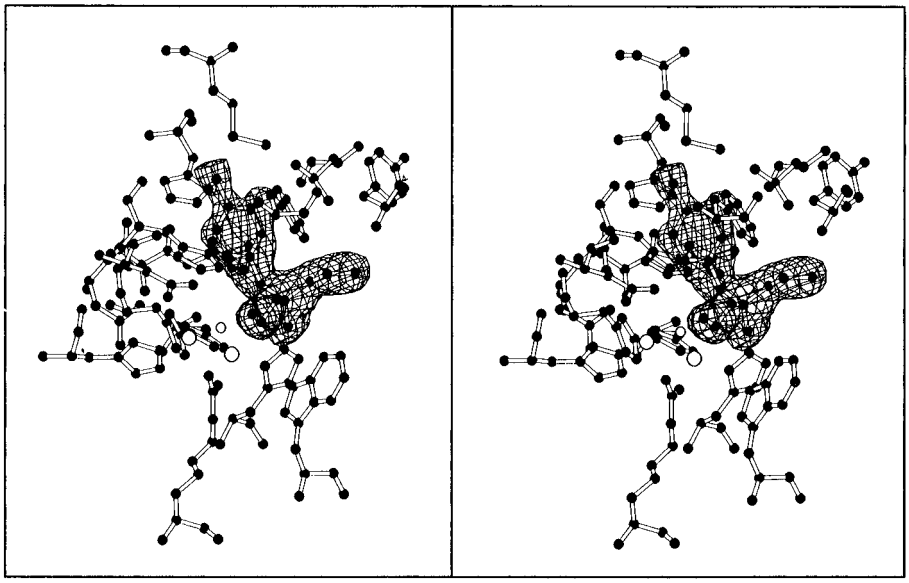

FIGURE 3: Electron density corresponding to diethyl 4-methylbenzylphosphonate in subunit II. The electron density shown was calculated to 2.1 Å resolution with coefficients of the form $(F_o - F_c)$, where F_o and F_c were the native and calculated structure factor amplitudes, respectively. The coordinates for the substrate analog were omitted in the calculation. The map was contoured at 3σ. The average *B*-values for the inhibitors in subunits I and II were 57 and 51 Å^2, respectively.

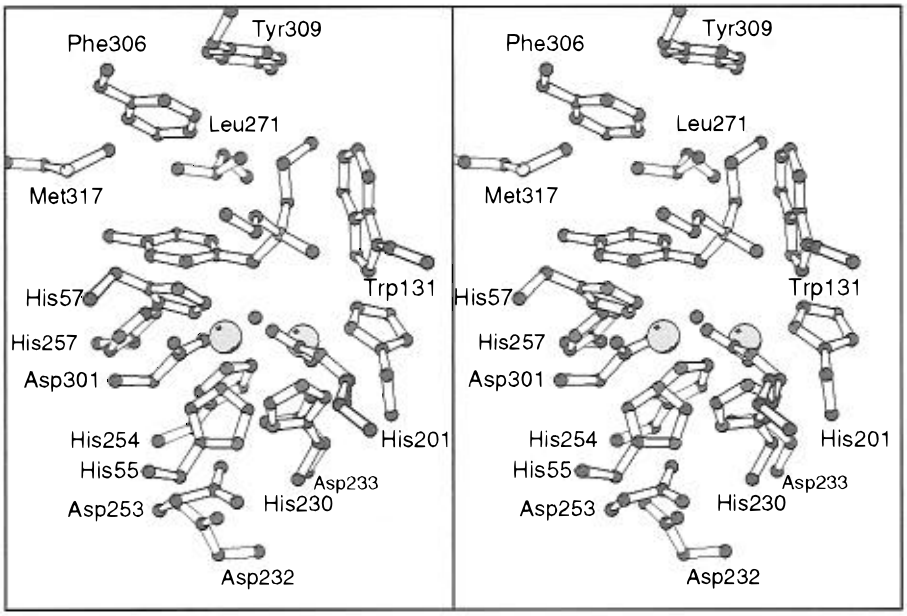

FIGURE 4: Close-up view of the active site for phosphotriesterase. Those amino acid residues that are located within approximately 3.5 Å of diethyl 4-methylbenzylphosphonate and the zinc ions are displayed.

form of phosphotriesterase, this ion is ligated in an octahedral arrangement by Lys 169, His 201, His 230, two water molecules, and the bridging hydroxide. In the model reported here, the zinc ion is surrounded by Lys 169, His 201, His 230 and the bridging hydroxide ion in a distorted tetrahedral environment with bond angles ranging from 91° to 111°. This difference in geometry about the second zinc ion may be a function of ligation preference or may result from the presence of the substrate analog bound in the active site. The atomic radii for Zn^{2+} and Cd^{2+} are 0.74 and 0.97 Å, respectively. It appears that the polypeptide chain backbone of phosphotriesterase provides a scaffold that easily accommodates such differences. This is further emphasized by the fact that all the protein atoms for these two forms of phosphotriesterase, including side chains, superimpose with a root-mean-square deviation of 0.40 Å.

The inhibitor employed in this investigation, diethyl 4-methylbenzylphosphonate, is as follows:

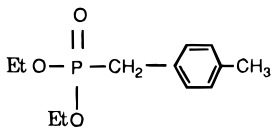

Electron density corresponding to this substrate analog is displayed in Figure 3, and as can be seen, the positioning of the molecule is unambiguous. A close-up view of the active site pocket is given in Figure 4. The binding pocket is characterized by a lack of hydrogen bonding between the protein and the inhibitor. The only specific electrostatic interactions that occur involve the phosphoryl oxygen of the analog, which is located at 3.3 Å from $N^{\epsilon 1}$ of Trp 131, 3.2 Å from $N^{\delta 1}$ of His 201, and 3.5 Å from the more solvent-

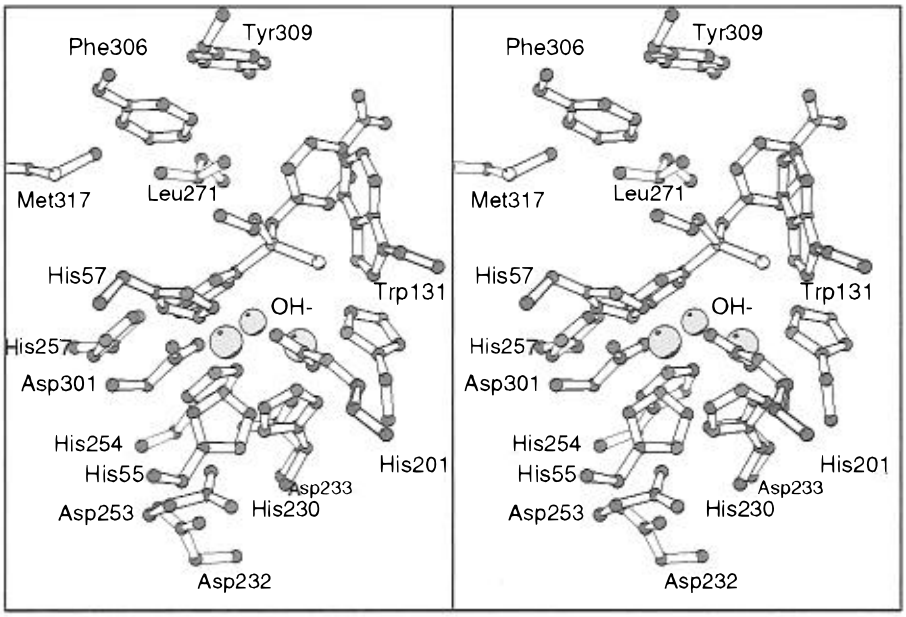

FIGURE 5: Putative mode of binding of the S_p-enantiomer of EPN to phosphotriesterase. The EPN analog was superimposed onto the coordinates of the diethyl 4-methylbenzylphosphonate with the *p*-nitrophenol group of EPN occupying the *pro-S* position of diethyl 4-methylbenzylphosphonate. For viewing purposes, the bridging hydroxide ion was enlarged to emphasize its position with respect to the phosphorus atom of the substrate. X-ray coordinates for EPN were determined by Gifkins and Jacobson (1980).

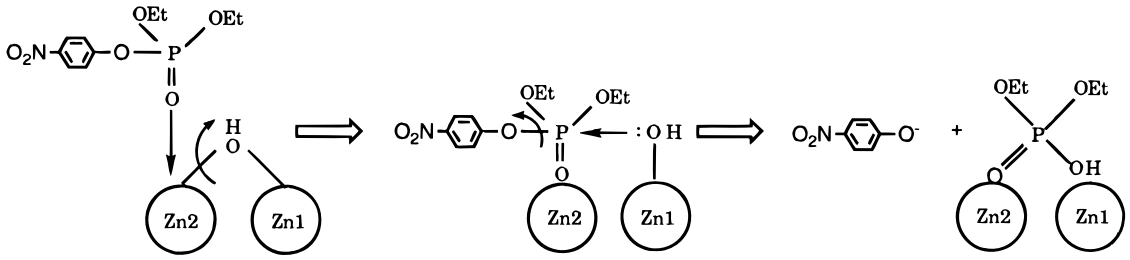

FIGURE 6: Schematic representation of the postulated catalytic mechanism of phosphotriesterase.

exposed zinc ion. The methylbenzyl group of the inhibitor sits in a fairly hydrophobic pocket defined by His 257, Leu 271, Phe 306, and Met 317. The phosphonate inhibitor employed in this investigation is prochiral. Each of the two enantiotopic ethoxy groups, however, occupies unique locations within the binding pocket of phosphotriesterase. The *pro-S* arm is pointed away from the binuclear metal center toward the solvent. Those amino acid residues closest to this ethoxy group are Trp 131, Phe 132, Leu 271, Phe 306, and Tyr 309. The *pro-R* ethoxy group is pointed toward amino acid residues Trp 131, Ile 160, Leu 303, Phe 306, and Ser 308.

The stereochemistry of the phosphotriesterase reaction is known to proceed with net inversion of configuration about the phosphorus center of the substrate (Lewis *et al.*, 1988). The reaction mechanism was therefore postulated to occur via an S_N2-type mechanism, whereby an activated water molecule attacks the electrophilic phosphorus of the substrate. Examination of the relative orientation of the metal-bound hydroxide reveals that the methylbenzyl group of the bound inhibitor is not located in the proper position to serve as a surrogate for the leaving group of a true substrate. Moreover, the aromatic group of this inhibitor is directed at the interior of the protein rather than toward the bulk solvent. It is known, however, that phosphotriesterase can hydrolyze a broad range of substrates including the S_p-enantiomer of EPN [*O*-ethyl *O*-(4-nitrophenyl)benzenephosphonothioate] (Lewis *et al.*, 1988):

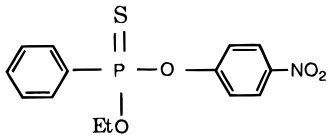

The R_p-isomer is not a substrate for the enzyme. We propose that the methylbenzyl group of the inert inhibitor is positioned within the active site at the location normally occupied by the phenyl substituent of EPN during productive catalysis. If the S_p-isomer of EPN is modeled into the active site of phosphotriesterase by first fixing the relative location of the phenyl group and the thiophosphoryl group as described above, then the *p*-nitrophenol leaving group would occupy the same general position as the *pro-S* ethoxy group of the phosphonate inhibitor. As shown in Figure 5, the *p*-nitrophenol leaving group is directed towards the solvent and is in the expected position relative to a nucleophilic attack by the bound metal hydroxide. It can thus be postulated that the activation of the nucleophilic water molecule occurs not via a traditional enzymatic base but rather through interactions with the binuclear metal center as shown schematically in Figure 6. According to a previously suggested model by Benning *et al.* (1995), the phosphoryl oxygen of the substrate binds to the less buried zinc ion, displacing the hydroxide ion from the first metal. The electrophilic phosphorus of the substrate is subsequently

attacked by the hydroxide, resulting in inversion of the stereochemistry about the phosphorus and expulsion of the aromatic leaving group from the open end of the β-barrel of the protein. The studies described here with diethyl 4-methylbenzylphosphonate lend further support to this mechanism.

Phosphotriesterase is unique among the organophosphate-degrading enzymes, such as the paraoxonases and the DFPases, in that it is capable of hydrolyzing both widely employed pesticides and phosphofluoridates such as sarin and soman. The model of the phosphotriesterase/diethyl 4-methylbenzylphosphonate complex described here represents the first direct visualization of a substrate analog bound in the active site pocket. Experiments designed to further investigate the chemical mechanism and the broad substrate specificity of the enzyme are presently in progress.

ACKNOWLEDGMENT

We thank Dr. Jane M. Kuo for the purification and preparation of the zinc-containing phosphotriesterase employed in this investigation. The helpful discussions of Dr. W. W. Cleland are gratefully acknowledged. In addition, we thank a reviewer for indicating the proper resonance structures for Figure 2.

REFERENCES

Benning, M. M., Kuo, J. M., Raushel, F. M., & Holden, H. M. (1994) *Biochemistry 33*, 15001−15007.
Benning, M. M., Kuo, J. M., Raushel, F. M., & Holden, H. M. (1995) *Biochemistry 34*, 7973−7978.
Chae, M. Y., Omburo, G. A., Lindahl, P. A., & Raushel, F. M. (1993) *J. Am. Chem. Soc. 115*, 12173−12174.
Dumas, D. P., Caldwell, S. R., Wild, J. R., & Raushel, F. M. (1989) *J. Biol. Chem. 264*, 19659−19665.
Dumas, D. P., Durst, H. D., Landis, W. G., Raushel, F. M., & Wild, J. R. (1990) *Arch. Biochem. Biophys. 277*, 155−159.
Gifkins, M. R., & Jacobson, R. A. (1980) *Cryst. Struct. Commun. 9*, 571.
Jabri, E., Carr, M. B., Hausinger, R. P., & Karplus, P. A. (1995) *Science 268*, 998−1004.
Jones, A. T. (1985) *Methods Enzymol. 115*, 157−171.
Kabsch, W. (1988a) *J. Appl. Crystallogr. 21*, 67−71.
Kabsch, W. (1988b) *J. Appl. Crystallogr. 21*, 916−924.
Kraulis, P. J. (1991) *J. Appl. Crystallogr. 24*, 946−950.
Lewis, V. E., Donarski, W. J., Wild, J. R., & Raushel, F. M. (1988) *Biochemistry 27*, 1591−1597.
Omburo, G. A., Kuo, J. M., Mullins, L. S., & Raushel, F. M. (1992) *J. Biol. Chem. 267*, 13278−13283.
Omburo, G. A., Mullins, L. S., & Raushel, F. M. (1993) *Biochemistry 32*, 9148−9155.
Tronrud, D. E., Ten Eyck, L. F., & Mathews, B. W. (1987) *Acta Crystallogr. A43*, 489−501.

BI960325L